

# Nonlinear sub-structuring applied to pseudo-dynamic tests on RC structures

F. Ragueneau, A. Souid, A. Delaplace & R. Desmorat  
*LMT-Cachan, ENS Cachan/CNRS/Univ.Paris 6, Cachan, France*

**ABSTRACT:** This paper aims at giving some insights within the pseudo-dynamics tests on reinforced concrete structures. Nonlinear substructuring is used making benefits of simplified finite element analysis based on multifibers beams theory approach. Continuum damage mechanics is used for the modelled structure allowing creating a realistic dynamic environment for the tested substructure.

## 1 INTRODUCTION

The comprehension of the ultimate behaviour of Civil Engineering structures subject to natural or industrial risks such as shocks, impacts, earthquake, explosions, etc can be handled in two ways: experimental testing and numerical modelling. In earthquake engineering, the major drawback remains in the experimental work. One has to deal with large scale structures subject to dynamic and complex loading. Classical tests are performed on shaking tables, allowing reproducing real or artificial earthquake, but with reproducibility difficulties and physical measurement limitations. To overcome these difficulties, the pseudo-dynamic or hybrid testing are under developments (Pegon & Pinto 2000). A combination between the numerical modelling (into which one can introduce the suitable model of material behaviour) and a test on parts of the structures can be made to better understand the structure response while benefiting from the substructuring technique. To numerically determine the inertia forces for performing static tests instead of dynamic ones leads to the so-called pseudo-dynamics (PSD) modelling. We describe and present the results for such PSD tests with sub-structuring technique carried out in nonlinear range. In fact, taking into account the nonlinear behaviour of the modelized structure is of major importance since the concomitant stiffness or eigen-frequency decrease change the whole response of the structure and so, the boundary conditions and loadings of the tested structure.

The tests were conducted for a two level reinforced concrete frame which is subjected to a real two components earthquake (horizontal and vertical). We present the use of computations for the

modelized and tested sub-structures in the PSD tests. Both an implicit and an explicit time integration schemes are used for the simulated parts in parallel with an explicit one used for the tested part (Souid *et al.* 2005). Tests results are used to identify and validate the nonlinear constitutive equations. For instance, a three dimensional damage model with induced damage anisotropy is described and used for quasi-brittle materials such as concrete. The quasi-static condition of the tests allows performing refined field measurements using the digital images correlation techniques. At the scale of a reinforced concrete beam, one can distinguish for different geometries and steel reinforcement ratio, the rupture kinematics and make easier numerical model identification.

## 2 PSEUDO-DYNAMIC TESTING

### 2.1 General scheme

Evaluation of the seismic response of a structural system is usually conducted using a shaking table. However, shaking-table experiments for large-scale structures are difficult, for instance due to table capacity limitations. An alternative way of testing full or large scale structures is the PSD testing (Shing and Mahin, 1984, Takanashi and Nakashima, 1987). The PSD testing is an experimental technique developed to evaluate the seismic performance of structure samples in a laboratory by means of computer-controlled simulation. It is an hybrid method, in which the structural displacements due to the earthquake are computed by using a stepwise integration procedure. Let us consider the dynamic equilibrium equation under seismic external acceleration

$a(t)$ :

$$\mathbf{M}\ddot{\mathbf{u}}(t) + \mathbf{C}\dot{\mathbf{u}}(t) + \mathbf{r}(t) = \mathbf{f}(t) = -\mathbf{M}\{\dot{\mathbf{u}}\}a(t) \quad (1)$$

where  $\mathbf{M}$ ,  $\mathbf{C}$  are the mass and damping matrices,  $\dot{\mathbf{u}}(t)$  and  $\ddot{\mathbf{u}}(t)$  are respectively the relative velocity and acceleration vectors at time  $t$ . Knowing variables at time  $t_n$  one can compute displacement and velocity at time  $t_{n+1}$  by using a numerical scheme. Only the  $\mathbf{r}(t)$  forces are experimentally measured. Numerical time discretization schemes belong to the Newmark family. Within the framework of experiment-computation interaction (Shing *et al.* 1991), an efficient and pragmatic choice consists in implementing an Operator Splitting algorithm, allowing for a direct integration without iteration in the linear range (Nakashima *et al.* 1993). In nonlinear regime up to rupture, it becomes necessary to damp the high frequencies, sources of numerical instabilities when an explicit procedure is adopted. In that purpose, the OS technique can be coupled to the HHT algorithm (Hilber *et al.* 1977, Combescure & Pegon 1997). Knowing the accelerogram and so the acceleration vector  $\ddot{\mathbf{u}}^{n+1}$ , the displacements and velocities are predicted as following

$$\mathbf{u}_{trial}^{n+1} = \mathbf{u}^n + \Delta t \dot{\mathbf{u}}^n + \frac{1}{2} \Delta t^2 (1 - 2\beta) \ddot{\mathbf{u}}^n \quad (2)$$

$$\dot{\mathbf{u}}_{trial}^{n+1} = \dot{\mathbf{u}}^n + \Delta t (1 - \gamma) \ddot{\mathbf{u}}^n \quad (3)$$

and corrected using:

$$\mathbf{u}^{n+1} = \mathbf{u}_{trial}^{n+1} + \Delta t^2 \beta \ddot{\mathbf{u}}^{n+1} \quad (4)$$

$$\dot{\mathbf{u}}^{n+1} = \dot{\mathbf{u}}_{trial}^{n+1} + \Delta t \gamma \ddot{\mathbf{u}}^{n+1} \quad (5)$$

with  $\beta = (1 - \alpha)^2 / 4$  et  $\gamma = (1 - 2\alpha) / 2$ . For  $\alpha = 0$ , we recover the classical Newmark scheme (1/2, 1/4) and for  $\alpha \in [-1/3; 0[$ , the numerical scheme dissipates energy. To get an explicit solution, one may approximate the stiffness forces by:

$$\mathbf{r}^{n+1}(\mathbf{u}^{n+1}) \approx \mathbf{K}^I \mathbf{u}^{n+1} + (\mathbf{r}_{trial}^{n+1}(\mathbf{u}_{trial}^{n+1}) - \mathbf{K}^I \mathbf{u}_{trial}^{n+1}) \quad (6)$$

$\mathbf{K}^I$  is a stiffness matrix (from the initial virgin one to the tangential one). Using the equation of motion at time  $n+1$  shifted of  $\alpha$ , one may obtain the acceleration vector by solving the linear algebraic system:

$$\widehat{\mathbf{M}} \ddot{\mathbf{u}}^{n+1} = \widehat{\mathbf{f}}^{n+1} \quad (7)$$

with  $\widehat{\mathbf{M}} = \mathbf{M} + \gamma \Delta t (1 + \alpha) \mathbf{C} + \beta \Delta t^2 (1 + \alpha) \mathbf{K}^I$  and:

$$\widehat{\mathbf{f}}^{n+1} = (1 + \alpha) \mathbf{f}^{n+1} - \alpha \mathbf{f}^n + \alpha \mathbf{r}_{trial}^{n+1} - (1 + \alpha) \mathbf{r}_{trial}^n + \alpha \mathbf{C} \dot{\mathbf{u}}_{trial}^n - (1 + \alpha) \mathbf{C} \dot{\mathbf{u}}_{trial}^{n+1} + \alpha (\gamma \Delta t \mathbf{C} + \beta \Delta t^2 \mathbf{K}^I) \ddot{\mathbf{u}}^n \quad (8)$$

## 2.2 Sub-structuring

The PSD testing with substructuring can significantly reduce the cost of the tests to get the seismic performance of the structures (Chung *et al.* 1999). In

substructuring technique, a physical model is built only on the part or parts where nonlinearity is expected (the physical substructure), with the remaining parts modeled computationally (the numerical substructure). This method initially developed by (Takanashi and Nakashima 1987), Mahin and Shing 1985) has been considerably extended by researchers at the JRC, (Buchet and Pegon 1994). The numerical part is simulated by using a finite element code in a computer connected through a network with other computers that realize the experimental procedures of the PSD test. The displacement at the interface between the physical and numerical substructures is obtained and applied to the test specimen by hydraulic actuators. The resulting resistance forces are measured by load cells and fed back to the numerical model, together with the next increment of earthquake ground motion. A new interface displacement is then calculated and applied to the tested specimen, and the loop is repeated until the test is completed, (Pegon & Pinto 2000, Chang 2001, Williams and Blakeborough 2001).

We denote by the subscripts  $S$  and  $T$  the matrices corresponding respectively to the simulated and the tested substructure. The  $i$  and  $j$  indices correspond to the internal nodes of the simulated substructure, the  $I$  and  $J$  indices to the internal nodes of the tested substructure and  $\delta$  and  $\theta$  to the interface nodes between the two substructures. Based on the equation 7, the system to solve sums up to:

$$\begin{bmatrix} {}^S \widehat{\mathbf{M}}_{ij} & {}^S \widehat{\mathbf{M}}_{i\theta} & 0 \\ {}^S \widehat{\mathbf{M}}_{\delta j} & {}^S \widehat{\mathbf{M}}_{\delta\theta} + {}^T \widehat{\mathbf{M}}_{\delta\theta} & {}^T \widehat{\mathbf{M}}_{\delta J} \\ 0 & {}^T \widehat{\mathbf{M}}_{I\theta} & {}^T \widehat{\mathbf{M}}_{IJ} \end{bmatrix} \begin{bmatrix} \ddot{\mathbf{u}}_j^{n+1} \\ \ddot{\mathbf{u}}_\theta^{n+1} \\ \ddot{\mathbf{u}}_J^{n+1} \end{bmatrix} = \begin{bmatrix} {}^S \widehat{\mathbf{f}}_i \\ {}^S \widehat{\mathbf{f}}_\delta + {}^T \widehat{\mathbf{f}}_\delta \\ {}^T \widehat{\mathbf{f}}_I \end{bmatrix} \quad (9)$$

A static condensation applied to interface nodes allows to treat only two systems: the first one for the simulated substructure and the second one for the tested substructure.

In order to account for the diffused cracking in the whole concrete structure, the nonlinear behaviour of materials has to be introduced in the simulated substructure as well. In order to ensure efficiency and robustness, the framework of simplified multifibres analysis has been chosen.

## 2.3 Numerical implementation and multifibres analysis

For a simple reason of excessive computational costs, complete 3D approaches to structural dynamics in civil engineering are not commonly used. Nonlinear dynamic analysis of complex civil engineering structures based on a detailed finite element model requires large scale computations and handles delicate solution techniques. The necessity to perform parametric studies due to the stochastic characteristic of the input accelerations imposes simplified numerical modeling which will reduce the computa-

tion cost. In classical multifibre analysis (Bazant *et al.* 1987, Spacone *et al.* 1996) the latter is achieved by selecting the classical Euler-Bernoulli beam model for representing the global behavior of the structural components of a complex civil engineering structure. With respect to the large spreading of the zone with nonlinear behavior it is further seek to limit the model complexity (and resulting computational costs) by limiting the diversity of possible deformation global patterns which is achieved in a multifibre beam model with fibres restricted to beam kinematics and with each one employing its own constitutive model (see figure 1). The main advantage of using a multifibre type finite element concerns the possibility to use a simple uniaxial behavior which allows for a very efficient implementation of nonlinear constitutive equations. This is no longer possible for thick beams where shear strains play a major role (Dubé 1994).

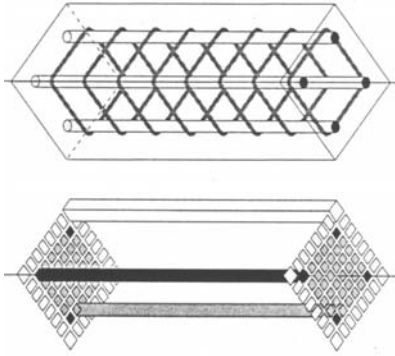


Figure 1. Multifibre mbeam for concrete structures (after Guedes *et al.* 1994)

The multifibre beam element developed herein employs the standard Hermite polynomial shape functions to describe the variation of the displacement field along the beam. For the Euler-Bernoulli element, the shear forces are computed at the element level through the equilibrium equations. Reinforcement bars are introduced as special fibres, whose behaviour is obtained as a combination of those for concrete and steel (mixture law). The difference with “classical” beam elements concerns the cross section behaviour, i.e. the relation between the generalized strains  $\mathbf{e}$  and the generalized stresses  $\mathbf{s}$ . In the general 3D case the latter includes:

$$\mathbf{s} = (N \quad M_x \quad M_y \quad M_z)^T \quad \text{and} \quad \mathbf{e} = (\varepsilon \quad \theta_x \quad \chi_y \quad \chi_z)^T \quad (10)$$

where  $N$  is the normal force,  $M_x$  the torque,  $M_y$  and  $M_z$  are the bending moments,  $\varepsilon$  the axial strain,  $\theta_x$  the twist,  $\chi_y$  and  $\chi_z$  the curvatures. The cross section behaviour is expressed with the constitutive matrix :

$$K = \begin{bmatrix} K_{11} & 0 & K_{13} & K_{14} \\ & K_{22} & 0 & 0 \\ & & K_{33} & K_{34} \\ \text{sym} & & & K_{44} \end{bmatrix} \quad (11)$$

where the coefficients are obtained by integration over the cross section (y and z axes) :

$$\begin{aligned} K_{11} &= \int_S E dS, \quad K_{13} = \int_S E z dS; \\ K_{14} &= -\int_S E y dS; \quad K_{22} = \int_S G (y^2 + z^2) dS \end{aligned} \quad (12)$$

$$K_{33} = \int_S E z^2 dS; \quad K_{34} = -\int_S E y z dS; \quad K_{44} = \int_S E y^2 dS$$

where  $E$  and  $G$  are Young's and shear moduli which vary in  $y$  and  $z$ . The chosen moduli can be initial, secant or tangent, depending upon the iterative algorithm used to solve the global equilibrium equations. The components of the constitutive matrix are computed by means of numerical integrations, often with one Gauss point per fibre. For the Euler-Bernoulli element, the shear forces are computed at the element level through the equilibrium equations (included in the Hermite polynomial shape functions).

When dealing with structures such as shear walls, which posses the slenderness ratio far from the classical beam ones, a more reliable representation of shear deformations and shear stresses has to be provided. One possibility in that respect is to use the classical Timoshenko beam model, which can describe the constant shear strain. The main difficulty of developing the finite element implementation of the Timoshenko beam model concerns the so-called shear locking phenomena, or inability of the standard finite element approximations to represent pure bending vanishing shear modes. A number of different remedies to shear locking problem has been proposed, ranging from selective or reduced integration, assumed shear strain, enhanced shear strain or hierarchical displacement interpolations. A recent work of Kotronis (2000) extends these ideas in order to construct shear locking remedies for a mulifibre Timoshenko beam.

### 3 CONCRETE MODELLING

Concerning the concrete constitutive equations, a refined modelling within the earthquake engineering scope should account for decrease in material stiffness as the microcracks open, stiffness recovery as crack closure occurs, inelastic strains concomitant to damage and induced anisotropy. The latter is obtained by an anisotropic damage model based on Continuum Damage Mechanics. The model is written within the thermodynamics framework and introduces only one damage 2<sup>nd</sup> order tensor variable. To describe the damage evolution, a damage criterion of Mazars (Mazars 1984) type is used. It introduces an equivalent strain computed from the positive part of the strain tensor. The numerical scheme used for the implementation in a F.E. code is implicit, with all the advantages of robustness and sta-

bility. However, the constitutive equations of the anisotropic damage can be solved in an exact way on an integration time step. The calculation of the damage and of the stress is then completely explicit from a programming point of view.

### 3.1 Elasticity-damage coupling

The damage state is represented by the 2nd order tensor  $\mathbf{D}$  and there is one known thermodynamics potential  $\rho\psi^*$  (Ladevèze 1983) from which derives a symmetric effective stress  $\tilde{\boldsymbol{\sigma}}$  independent from the elasticity parameters (Lemaitre & Desmorat 2000) :

$$\rho\psi^* = \frac{1+\nu}{2E} \text{Tr} \left[ (\mathbf{I}-\mathbf{D})^{-1/2} \boldsymbol{\sigma}_+^D (\mathbf{I}-\mathbf{D})^{-1/2} \boldsymbol{\sigma}_+^D + \langle \boldsymbol{\sigma}^D \rangle_-^2 \right]_+ + \frac{1-2\nu}{6E} \left[ \frac{\langle \text{Tr} \boldsymbol{\sigma} \rangle_+^2}{1-D_H} + \langle -\text{Tr} \boldsymbol{\sigma} \rangle_+^2 \right] \quad (13)$$

with  $E$ ,  $\nu$  the Young modulus and Poisson ratio of initially isotropic elasticity and  $\boldsymbol{\sigma}^D = \boldsymbol{\sigma} - 1/3 \text{Tr}[\boldsymbol{\sigma}] \mathbf{I}$  is the deviatoric stress and where  $D_H$  the hydrostatic damage  $D_H = 1/3 \text{Tr} \mathbf{D}$ .

Quasi-brittle materials such as concrete exhibit a strong difference of behavior in tension and in compression due to damage. This micro-defects closure effect usually leads to complex models when damage anisotropy is considered (Ladevèze 1983, Chaboche 1993, Dragon et Halm 1996) and the purpose here is to show that it is important for cyclic applications to consider damage anisotropy with a quasi-unilateral effect acting on the hydrostatic stress and on the deviatoric one. The thermodynamics potential writes:

$$\rho\psi^* = \frac{1+\nu}{2E} \text{Tr} \left[ (\mathbf{I}-\mathbf{D})^{-1/2} \boldsymbol{\sigma}_+^D (\mathbf{I}-\mathbf{D})^{-1/2} \boldsymbol{\sigma}_+^D + \langle \boldsymbol{\sigma}^D \rangle_-^2 \right]_+ + \frac{1-2\nu}{6E} \left[ \frac{\langle \text{Tr} \boldsymbol{\sigma} \rangle_+^2}{1-\text{Tr} \mathbf{D}} + \langle -\text{Tr} \boldsymbol{\sigma} \rangle_+^2 \right] \quad (14)$$

$\langle \cdot \rangle_-$  corresponds to the negative part of a tensor, expressed in its eigen-coordinates. In order to keep differentiability properties of the Gibbs free energy, the positive part  $\boldsymbol{\sigma}_+^D$  of  $\boldsymbol{\sigma}^D$  has to be carefully built (Ladevèze 1983). The following eigenvalue problem (eigenvalues  $\lambda^I$  and corresponding eigenvectors  $\tilde{T}^I$ ) has to be solved :

$$\boldsymbol{\sigma}_+^D \tilde{T}^I = \lambda^I (\mathbf{I}-\mathbf{D})^{1/2} \tilde{T}^I \quad (15)$$

The norm being defined as :  $\tilde{T}^{IT} (\mathbf{I}-\mathbf{D})^{1/2} \tilde{T}^J = \delta_{IJ}$ . The positive part of the deviator is then expressed as:

$$\boldsymbol{\sigma}_+^D = \sum_{I=1}^3 [(\mathbf{I}-\mathbf{D})^{1/2} \tilde{T}^I] [(\mathbf{I}-\mathbf{D})^{1/2} \tilde{T}^I]^T \langle \lambda^I \rangle_+ \quad (16)$$

The elasticity law reads

$$\boldsymbol{\varepsilon} = \rho \frac{\partial \psi^*}{\partial \boldsymbol{\sigma}} = \frac{1+\nu}{E} \text{Tr} \left[ \left[ (\mathbf{I}-\mathbf{D})^{-1/2} \boldsymbol{\sigma}_+^D (\mathbf{I}-\mathbf{D})^{-1/2} \right]^D + \langle \boldsymbol{\sigma}_-^D \rangle_-^D \right] + \frac{1-2\nu}{3E} \left[ \frac{\langle \text{Tr} \boldsymbol{\sigma} \rangle_+}{1-\text{Tr} \mathbf{D}} - \langle -\text{Tr} \boldsymbol{\sigma} \rangle_+ \right] \mathbf{I} \quad (17)$$

$$= \frac{1+\nu}{E} \tilde{\boldsymbol{\sigma}} - \frac{\nu}{E} \text{Tr} \tilde{\boldsymbol{\sigma}} \mathbf{I}$$

and defines the symmetric effective stress  $\tilde{\boldsymbol{\sigma}}$  independent from the elasticity parameters, :

$$\tilde{\boldsymbol{\sigma}} = [(\mathbf{I}-\mathbf{D})^{-1/2} \boldsymbol{\sigma}_+^D (\mathbf{I}-\mathbf{D})^{-1/2}]^D + \langle \boldsymbol{\sigma}_-^D \rangle_-^D + \frac{1}{3} \left[ \frac{\langle \text{Tr} \boldsymbol{\sigma} \rangle_+}{1-\text{Tr} \mathbf{D}} - \langle -\text{Tr} \boldsymbol{\sigma} \rangle_+ \right] \mathbf{I} \quad (18)$$

The notation  $\langle x \rangle_+$  stands for the positive part of a scalar,  $\langle x \rangle_+ = x$  if  $x > 0$ ,  $\langle x \rangle_+ = 0$  else.

### 3.2 Damage threshold function

As for plasticity, the elasticity domain can be defined through a criterion function  $f$  such as the domain  $f < 0$  corresponds to elastic loading or unloading. Many criterion can be used, written in terms of stresses such as plasticity criteria, strains, or strain energy release rate density leading or not to dilatancy in compression. The purpose here is to build a constitutive model with a restricted number of material parameters, robust and easy to implement in Finite Element computer codes. Dilatancy will not be taken into account and one will accept an open criterion for the tricompression states. These remarks lead us to the simple choice of Mazars criterion, function of the positive extensions  $\langle \varepsilon_I \rangle$  of the  $I$ th principal strain  $\varepsilon_I$ ,

$$f = \hat{\varepsilon} - \kappa(\text{tr} \mathbf{D}) \quad \text{with} \quad \hat{\varepsilon} = \sqrt{\langle \boldsymbol{\varepsilon} \rangle_+ : \langle \boldsymbol{\varepsilon} \rangle_+} = \sqrt{\sum \langle \varepsilon_I \rangle^2} \quad (19)$$

where  $\hat{\varepsilon}$  is the equivalent strain for quasi-brittle materials and  $\kappa$  is the elastic strain limit in tension. Different expressions for the equivalent strain may be adopted, allowing dealing with biaxial behaviour in a more appropriate way. For example, one can consider the de Vree (de Vree *et al.* 1995) formulation :

$$\hat{\varepsilon} = \frac{k-1}{2k(1-2\nu)} I_1 + \frac{1}{2k} \sqrt{\frac{(k-1)^2}{(1-2\nu)^2} I_1^2 - \frac{12k}{(1+\nu)^2} J_2} \quad (20)$$

with  $I_1 = \text{Tr} \boldsymbol{\varepsilon}$  and  $J_2 = 1/6 I_1^2 - 1/2 \boldsymbol{\varepsilon} : \boldsymbol{\varepsilon}$ . The biaxial response of anisotropic modelling using Mazars or de Vree equivalent strain is given in figure 2 and 3.

### 3.3 Damage evolution laws

To propose a damage model written in the thermodynamics framework, consider a damage pseudopotential  $F = Y : \langle \boldsymbol{\varepsilon} \rangle_+$  where  $\boldsymbol{\varepsilon}$  acts as a parameter so that the damage evolution law is derived from the normality rule as

$$\dot{\mathbf{D}} = \dot{\lambda} \frac{\partial F}{\partial \mathbf{Y}} = \dot{\lambda} \langle \boldsymbol{\varepsilon} \rangle_+ \quad (21)$$

The damage multiplier  $\lambda$  is determined from the consistency condition  $f = 0$ ,  $\dot{f} = 0$ . with  $f = \hat{\varepsilon} - \kappa(\xi)$ , and,  $\xi = \frac{\mathbf{D} : \langle \boldsymbol{\varepsilon} \rangle_+}{\max(\varepsilon_I)}$ .

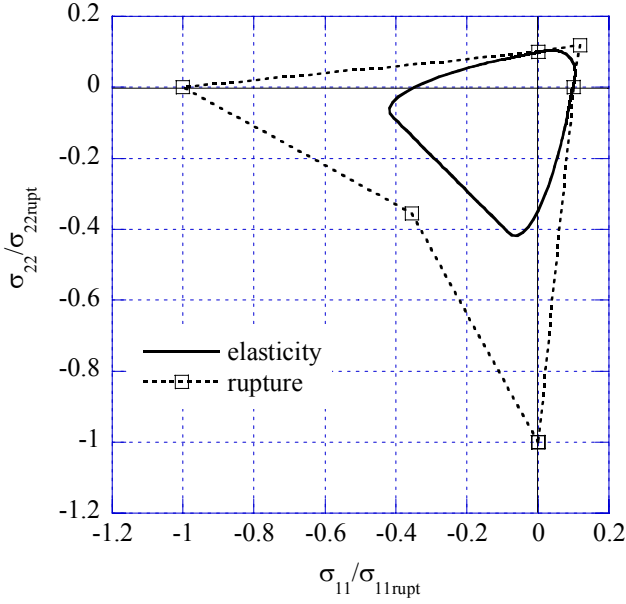


Figure 2. Elasticity and rupture for the Mazars equivalent strain.

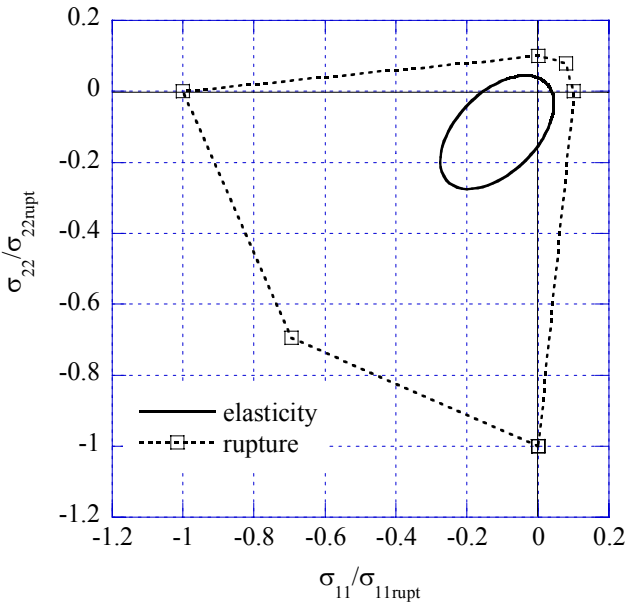


Figure 3. Elasticity and rupture for the de Vree equivalent strain.

Concerning the consolidation function  $\kappa$  to account for damage increase in tension as well as in compression, a possible choice is:  $\kappa = \kappa(\xi)$ . One has still to define the function  $\kappa$ . The simplest choice is to consider a linear function introducing two parameters only (law 1): the damage threshold  $\kappa_0 = \kappa(0)$  and a damage parameter  $A$  as

$$\kappa(\mathbf{D}) = \frac{1}{A}(\xi) + \kappa_0 \quad (22)$$

Damage anisotropy is different in tension and in compression. It affects differently the elasticity law and a strong difference in tension and in compression is finally obtained with the quite simple damage evolution law 1 (figure 1). Important point, this feature is gained with the consideration of one (tensorial) damage variable only in accordance with the thermodynamic definition of a state variable: if one degradation mechanism is observed, only one damage variable shall represent the micro-cracks or micro-defects pattern, whatever the material is in tension or in compression. The dissymmetry is nevertheless not sufficient with the linear  $\kappa$ -function with a too high damage rate in compression leading to a non physical snapback. One prefers then to consider as damage evolution law:

$$\dot{\mathbf{D}} = \frac{d\kappa^{-1}}{d\hat{\varepsilon}} \frac{\langle \boldsymbol{\varepsilon} \rangle_+}{\hat{\varepsilon}} \dot{\hat{\varepsilon}} = A \left[ 1 + \frac{\hat{\varepsilon}^2}{a^2} \right]^{-1} \frac{\langle \boldsymbol{\varepsilon} \rangle_+}{\hat{\varepsilon}} \dot{\hat{\varepsilon}} \quad (23)$$

with  $a$  a material parameter of the order of magnitude the value of the strain reached in compression. This defines  $\kappa^{-1}$  and  $\kappa$  as

$$\kappa(\xi) = a \cdot \tan \left[ \frac{\xi}{aA} + \arctan \left( \frac{\kappa_0}{a} \right) \right] \quad (24)$$

### 3.4 Model responses

Using the following material parameters ( $E = 42$  GPa,  $\nu = 0.2$ ,  $\kappa_0 = 5 \cdot 10^{-5}$ ,  $A = 5 \cdot 10^3$ ,  $a = 2.93 \cdot 10^{-4}$ ), the uniaxial response of the model is given in figure 4 for compression loading. The cyclic behaviour is presented in figure 5. The unilateral behaviour as well as the damage deactivation when passing from tension to compression are recovered.

### 3.5 Numerical implementation

The anisotropic damage model is in fact quite simple to implement in a FE code. A global resolution of the equilibrium equations gives the displacements at time  $t_{n+1}$  with the internal damage variable  $\mathbf{D} = \mathbf{D}_{n+1}$  kept unchanged from the last computed increment  $t_n$ . The strains  $\boldsymbol{\varepsilon}_{n+1}$  at each Gauss point are calculated from the elements interpolation functions. To integrate the constitutive equations means to determine the stress  $\boldsymbol{\sigma}_{n+1}$  and the damage  $\mathbf{D}_{n+1}$  at time  $t_{n+1}$ . An iterative process, not described here, made of global equilibrium resolutions followed by local time integration of the constitutive equations often takes place. One focuses here on the numerical scheme for the local integration of the damage law.

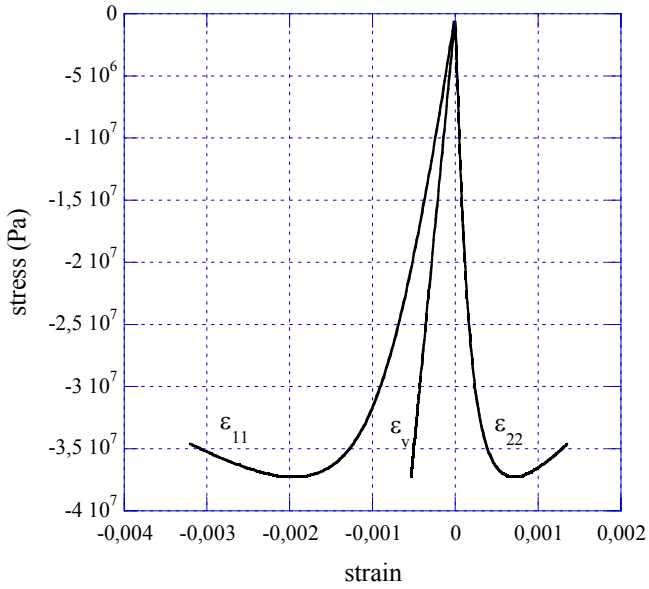


Figure 4. 3D model response in compression.

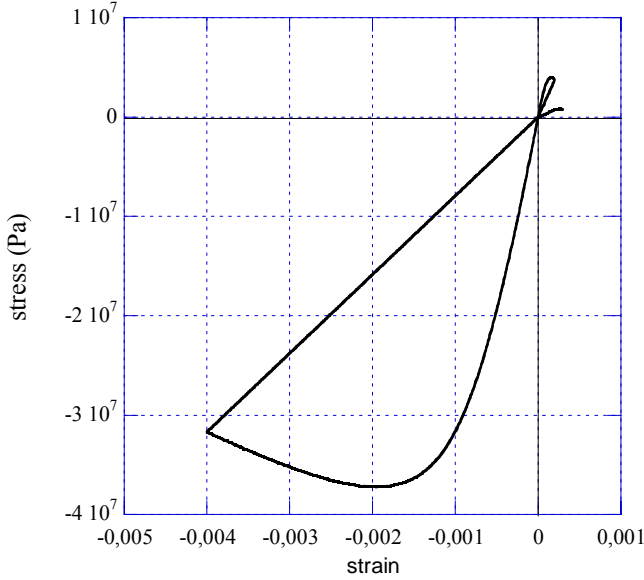


Figure 5. Cyclic uniaxial model response Tension - Compression - Tension.

Compute the equivalent strain :

$$\hat{\varepsilon}_{n+1} = \sqrt{\langle \boldsymbol{\varepsilon}_{n+1} \rangle_+ : \langle \boldsymbol{\varepsilon}_{n+1} \rangle_+} \quad (25)$$

Make a test on the criterion function :

$$f = \hat{\varepsilon}_{n+1} - \kappa(\mathbf{D}_n) \quad (26)$$

If  $f \leq 0$ ,  $\mathbf{D}_{n+1} = \mathbf{D}_n$  (material behaves elastically), else the damage must be corrected by using the damage evolution law discretized as

$$\Delta \mathbf{D} = \mathbf{D}_{n+1} - \mathbf{D}_n = \Delta \lambda \langle \boldsymbol{\varepsilon}_{n+1} \rangle_+ \quad (27)$$

The damage multiplier is determined from the consistency condition numerically written  $f_{n+1} = \hat{\varepsilon}_{n+1} - \kappa(\mathbf{D}_{n+1}) = 0$  so that

$$\Delta \lambda = \frac{\mathbf{D}_{n+1} : \langle \boldsymbol{\varepsilon}_{n+1} \rangle_+ - \mathbf{D}_n : \langle \boldsymbol{\varepsilon}_n \rangle_+}{\hat{\varepsilon}_{n+1}^2} \quad (28)$$

with  $\mathbf{D}_{n+1} : \langle \boldsymbol{\varepsilon}_{n+1} \rangle_+ = \left| \max \langle \varepsilon_I \rangle_+ \right| \kappa^{-1}$  being known and the exact actualisation of  $\mathbf{D}$  :

$$\mathbf{D}_{n+1} = \mathbf{D}_n + \Delta \lambda \langle \boldsymbol{\varepsilon}_{n+1} \rangle_+ \quad (29)$$

Stresses computation : Using the elasticity law allow for the computation of the effective stress tensor ( $\mathbf{E}$  is the elastic Hooke tensor),

$$\tilde{\boldsymbol{\sigma}}_{n+1} = \mathbf{E} : \boldsymbol{\varepsilon}_{n+1} \quad (30)$$

The stress tensor is obtained through the relation between the effective stress tensor and the stress tensor in an anisotropic framework (equation 18).

The numerical scheme is fully implicit, therefore robust, but it has the main advantage of the explicit schemes: there is no need of a local iterative process as the exact solution of the discretized constitutive equations can be explicitated (Desmorat *et al.* 2004).

#### 4 EXPERIMENTAL TESTS ON RC STRUCTURES

A full nonlinear pseudo-dynamic test with substructuring is proposed. A reinforced concrete structure, shown in figure 6 is considered. The clamped frame is loaded with a dynamic seismic signal applied on its foundation. The damage model is applied for concrete material, and a nonlinear plastic behaviour is chosen for steel bars. Computational time is limited in the following by taking into account a multifibre model with the Finite Element Code CAST3M. A distributed loading mass  $m$  is applied on the upper beam and on the right middle one. A concentrated loading mass  $M$  is applied in the middle of the left beam, with  $M \gg m$ . The frame failure is supposed to occur after the rupture of the left beam, as a low level of damage occurs in the rest of the structure. Then, just the left beam is tested and its stiffness is obtained experimentally (Laborderie 1991) as the response of the rest of the structure is computed. An additional condition is applied on the structure: horizontal displacements of the beam ends are equal. By the way, just a single degree of freedom is controlled on experimental setup. This assumption is valid in that case, where horizontal stiffness is much greater than the vertical one. The experimental set-up for testing RC beams under cyclic three points bend test is presented in figure 7.

A first experimental result is presented in figure 8, it shows the vertical displacement of the centre of the beam during the first seconds of the signal. The realization of quasi-static tests enables us to perform more precise measurements than in the case of tests in dynamics. At critical states of the seismic structural response, it is possible to carry out field meas-

urements via digital images correlation (Hild 2002). First results of this type are presented for three moments of the response: at the beginning of the earthquake, for a maximum negative moment and for a maximum positive moment. Placed at one third of the beam, the camera makes it possible to observe cracks openings in shear. Figure 9 presents the field of horizontal displacement. Openings of cracks from 50 to 700 microns thus could be observed at various instants.

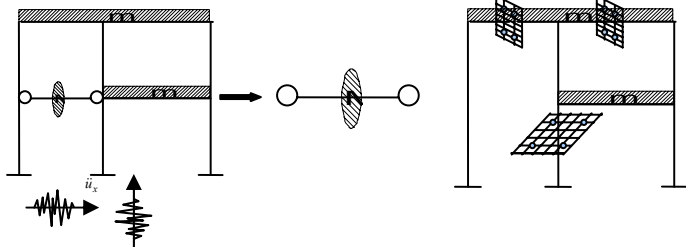


Figure 6. Substructuring decomposition for the nonlinear testing.



Figure 7. Experimental set-up for cyclic three points bend tests on RC beams.

## 5 CONCLUSIONS

Pseudo-dynamic tests with substructuring allow dynamic studies of large structures with a moderate experimental setup. Inertia forces are computed and the critical part of the structure is statically tested, while the non-critical parts of the structure are modeled. Based on this approach, our work focuses particularly on the damage model used for the modeled parts of the structure, and on the experimental measurements of damage on the tested structure. After a recall of the PSD test basis, we introduce an anisotropic damage model, based on a second order damage tensor, allowing describing induced anisotropy and crack closure with just five parameters. This model is used in the study of a reinforced concrete clamped frame, loaded with a seismic signal. One overloaded beam of the frame is experimentally tested, as the rest of the structure is modeled. Digital image correlation technique is used to study crack apparition and closure, allowing a fine identification and validation of the damage model. Experimental results validate the necessity to take into

account the low damage level of the non-critical parts.

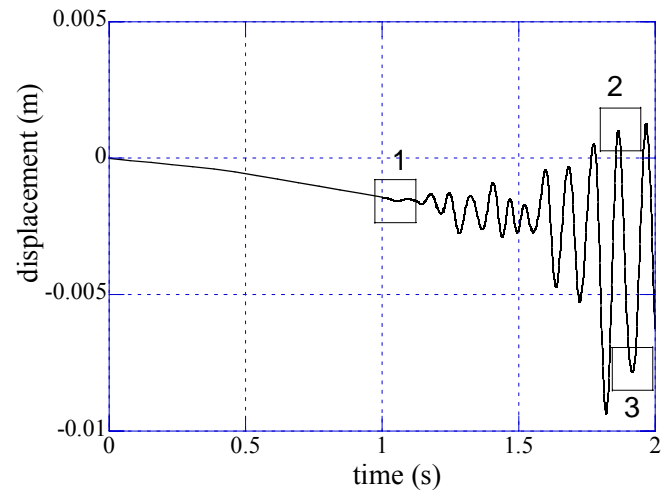


Figure 8. Experimental mid-span deflection.

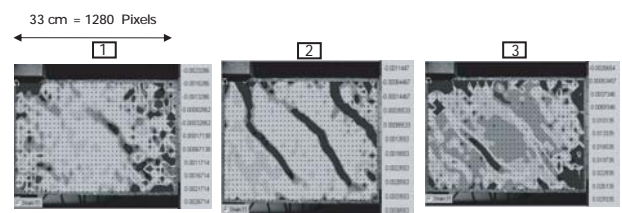


Figure 9. Results of digital image correlation analysis performed on the tested RC beams

## REFERENCES

- Bazant, Z.P., Pan J.-Y., Pijaudier-Cabot, G., 1987, Softening in reinforced concrete beams and frames, *ASCE J. of Struct. Engrg.* 113(12), pp. 2333-2347.
- Buchet, P. & Pegon, P., 1994, PSD testing with substructuring implementation and use, special publication, 1.94.25 JRC ISPRA
- Chaboche, J.L., 1993, Development of continuum Damage Mechanics for elastic solids sustaining anisotropic and unilateral damage, *Int. J. Damage Mechanics*, Vol. 2, pp. 311-329.
- Chang, S.Y., 2001, Application of the momentum equation of motion to pseudo-dynamic testing, *Phil. Trans. R. Soc. London*, 359, 1801-1827
- Chung, J., Yun, C.B., Kim, A.S. & Seo, J.W., 1999, Shaking table and pseudo dynamic tests for the evaluation of the seismic performance of base-isolated structure, *Engng. Struct.*, 21, 365-379
- Combescur, D. & Pegon, P., 1997,  $\alpha$ -Operator splitting time integration technique for pseudo-dynamic testing – error propagation analysis, *Soil Dynamics and Earthquake Engineering*, Vol. 16, pp. 427-443.
- de Vree J., Brekelmans W. & van Gils M., 1995. Comparison of nonlocal approaches in continuum damage mechanics, *Comp. Struct.* 55: 581-588
- Desmorat, R., Gatuingt, F., Ragueneau, F., 2004, Explicit evolution law for anisotropic damage : application to concrete structures, *NATO conf.*, Bled, Slovénie, juin 2004.
- Dragon, A., Halm, D., 1996, Modélisation de l'endommagement par mésosfissuration: comportement unilatéral et anisotropie induite, *C. R. Acad. Sci.*, t. 322, Série IIB, p. 275-282.
- Dubé, J. F., 1994, Modélisation simplifiée et comportement visco-endommageable des structures en béton, Ph. D. thesis: E.N.S.- Cachan

- Hilber, H.M., Hughes, T.J.R. & Taylor, R.L., 1977, Improved numerical dissipation for time integration algorithms in structural dynamics, *Earthquake Engineering Structural Dynamics*, vol. 5, pp. 283-292.
- Hild F., 2002, CORRELI<sup>LMT</sup>: a software for displacement field measurements by digital image correlation, Internal report N° 254. LMT-Cachan.
- Kotronis, P., 2000, Cisaillement dynamique de murs en béton armé. Modèles simplifiés 2D et 3D. Ph. D. thesis: ENS-Cachan.
- Laborderie C., 1991, Phénomènes unilatéraux dans un matériau endommageable, PhD thesis University Paris 6.
- Ladevèze, P., 1983, On an anisotropic damage theory, Proc. CNRS Int. Coll. 351 Villars-de-Lans, Failure criteria of structured media, Edited by J. P. Boehler, pp.355-363.
- Lemaitre, J. & Desmorat, R., 2005, Engineering Damage Mechanics: Ductile, Creep, Fatigue and Brittle Failures, Springer.
- Mahin, S. and Shing, P.B., 1985, Pseudodynamic method for seismic testing, *Struct. Eng.*, 111, 1482-1503
- Mazars, J., 1984, Application de la mécanique de l'endommagement au comportement non linéaire et à la rupture du béton de structure, Thèse d'état Université Paris 6.
- Nakashima, M., Akazawa, T. & Sakaguchi, O., 1993, Integration method capable of controlling experimental error growth in substructure pseudo-dynamic test. *Journal of Structural and Construction Engineering AIJ*, 454, pp. 61-71.
- Pegon, P. & Pinto, A.V., 2000, Pseudo-dynamic testing with substructuring at the elsa laboratory. *Earthquake Engng. Struct.Dyn* 29 905.925.
- Shing, P.B. & Mahin, S.A., 1984, Pseudodynamic method for seismic performance testing: theory and implementation. *UCB/ERC-84/01, Earthquake Engineering Research Centre*, University of California, Berkeley.
- Shing, P.B., Vannan, M.T. & Cater, E., 1991, Implicit time integration for pseudodynamic Pegon tests. *Earthquake Engineering Structural Dynamics*, Vol. 20, pp. 551-576.
- Soud, A. Delaplace, A., Ragueneau, F. and Desmorat, R., 2005, Pseudodynamic tests and substructuring of damageable structures, Sixth European Conference on Structural Dynamics, Paris, France.
- Spacone, E., Filippou, F.C. & Taucer, F.F., 1996, Fiber Beam-Column Model for Nonlinear Analysis of R/C Frames. I: Formulation. *Earthquake Engineering and Structural Dynamics*, Vol. 25, N. 7., pp. 711-725.
- Takanashi, K. and Nakashima, M., 1987, Japanese activities online testing, *Engng. Mech.*, 113, 1014-1032.
- Williams, M.S. & Blakeborough, A. 2001, Laboratory testing of structures under dynamic loads: an introductory review., *Phil. Trans. R. Soc. Lond.*, 1651-1669.